CHAPTER

3

Micropatterning Hydroxy-PAAm Hydrogels and Sylgard 184 Silicone Elastomers with Tunable Elastic Moduli

Marie Versaevel[1], Thomas Grevesse[1], Maryam Riaz, Joséphine Lantoine, and Sylvain Gabriele

Mechanobiology and Soft Matter Group, Laboratoire Interfaces et Fluides Complexes, Complexys and Biosciences Research Institutes, CIRMAP, Université de Mons, Mons, Belgium

[1]These authors contributed equally

CHAPTER OUTLINE

Methods in Cell Biology, Volume 121 **ISSN 0091-679X**

http://dx.doi.org/10.1016/B978-0-12-800281-0.00003-8

Abstract

This protocol describes a simple method to deposit protein micropatterns over a wide range of culture substrate stiffness (three orders of magnitude) by using two complementary polymeric substrates. In the first part, we introduce a novel polyacrylamide hydrogel, called hydroxy-polyacrylamide (PAAm), that permits to surmount the intrinsically nonadhesive properties of polyacrylamide with minimal requirements in cost or expertize. We present a protocol for tuning easily the rigidity of "soft" hydroxy-PAAm hydrogels between ~0.5 and 50 kPa and a micropatterning method to locally deposit protein micropatterns on these hydrogels. In a second part, we describe a protocol for tuning the rigidity of "stiff" silicone elastomers between ~100 and 1000 kPa and printing efficiently proteins from the extracellular matrix. Finally, we investigate the effect of the matrix rigidity on the nucleus of primary endothelial cells by tuning the rigidity of both polymeric substrates. We envision that the complementarity of these two polymeric substrates, combined with an efficient microprinting technique, can be further developed in the future as a powerful mechanobiology platform to investigate *in vitro* the effect of mechanotransduction cues on cellular functions, gene expression, and stem cell differentiation.

INTRODUCTION

It is now widely accepted that the mechanical environment plays an important role in directing cell fate and tissue morphogenesis (Guilak et al., 2009; Lecuit & Lenne, 2007). Several reports have demonstrated that cells undergo drastic morphological changes in response to external forces (e.g., shear stress, compression, or stretch) and modifications of the physicochemical properties of the extracellular matrix (ECM) (e.g., durotaxis, chemotaxis, or haptotaxis). The cell microenvironment presents narrow pores that impose a confined adhesiveness, which in turn influences the cellular shape and cytoskeletal organization (Gabriele, Benoliel, Bongrand, & Théodoly, 2009; Gabriele, Versaevel, Preira, & Théodoly, 2010; Pathak & Kumar, 2012). These stimuli are translated in adherent cells into a cascade of biochemical events through complex mechanotransduction pathways (Jaalouk & Lammerding, 2009). In this context, recent works have suggested the existence of a mechanical coupling between the ECM and the nucleus (Versaevel, Grevesse, & Gabriele, 2012;

Versaevel, Grevesse, Riaz, & Gabriele, 2013; Wang, Tytell, & Ingber, 2009) that may explain how modifications of the ECM can alter the gene machinery. The elucidation of the signaling pathways underlying the regulation of cellular shapes and nuclear functions requires the identification of intracellular components that are specifically activated in response to different ECM cues.

To tackle this problem, various natural and synthetic *in vitro* platforms have been refined and created to reproduce the complexity of the ECM. Indeed, most of the experiments in the field of mechanobiology were performed until recently in plastic dishes, which represent a physiologically inappropriate environment. As the importance of the mechanical properties of the ECM has been realized, researchers have started to develop synthetic materials that can recapitulate the range of physiological ECM rigidities. Some of these works have revealed that migration of 3T3 fibroblasts and rat kidney epithelial cells is regulated by the ECM stiffness (Pelham & Wang, 1997), that fibroblasts tune their internal stiffness to match that of the ECM (Solon, Levental, Sengupta, Georges, & Janmey, 2007), and that changes in the ECM stiffness can drive the differentiation of mesenchymal stem cells into specific lineages (Engler, Sen, Sweeney, & Discher, 2006).

By combining these novel materials with elegant microprinting technologies, biologically relevant questions have been recently assessed via the creative design of well-defined microenvironments. For instance, researchers have sought to develop a diverse set of complex microenvironments to probe the complexity of cell–substrate interactions in cellular motility (Brock et al., 2003; Théry, 2010), differentiation (Gao, McBeath, & Chen, 2010), or cell division (Kwon et al., 2008; Théry et al., 2005). Among these works, many efforts have been directed toward understanding the relationship between cell shape and nuclear functions (Thomas, Collier, Sfeir, & Healy, 2002; Versaevel et al., 2012, 2013) and decoupling the effect of the matrix stiffness on nuclear mechanotransduction (Grevesse, Versaevel, Circelli, Desprez, & Gabriele, 2013).

Most of cell types exhibit an elastic modulus in the range of ~1 to ~100 kPa, but there are also some tissues that experience a stiffer environment (Palchesko, Zhang, Sun, & Feinberg, 2012), such as cardiac muscle tissues (~40–400 kPa), arterial walls (~800 kPa), or basement membranes (~1–3 MPa). However, only very few materials have been reported to be able to cover the entire range of soft elastic moduli (from kPa to MPa) that can be found in the human body. To address this challenge, we describe how microcontact printing can be easily combined with modified polyacrylamide hydrogels for creating modified "soft" (0.5–50 kPa) culture substrates and silicone elastomers for modified "stiff" (~100 kPa–1 MPa) matrices (Fig. 3.1).

3.1 PHOTOMASK AND MICROSTAMPS

The microcontact printing technique requires the design of a photomask in a drawing software that can be open source (e.g., FreeCAD or LibreCAD) or commercial (e.g., Clewin or Autocad). These softwares allow to draw mask features with a micrometer

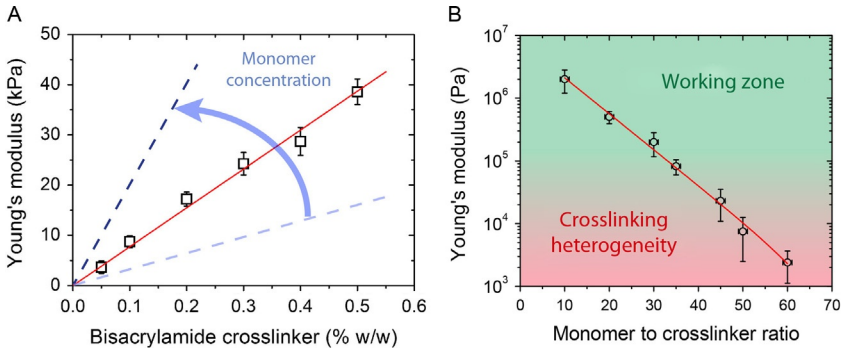

FIGURE 3.1

Elasticity of hydroxy-PAAm hydrogels and silicone gels. (A) Hydroxy-PAAm hydrogel elasticity versus bis-acrylamide cross-linker concentration (in w/w %). The linear fit (red line) shows the linear evolution of the elasticity with the cross-linker ratio, whereas dashed blue lines (light and dark) indicate that the range of elastic moduli can be adjusted by changing the monomer concentration. (B) The linear evolution of the Young's modulus of the Sylgard 184 as a function of monomer to cross-linker ratio indicates that varying the cross-linking density of Sylgard 184 allows to tailor the mechanical properties of the substrate. Variability in the Young's modulus increased in very soft samples (from 40:1 to 60:1) and may have resulted from cross-linking heterogeneity. The green region corresponds to the working area, whereas the red region corresponds to the presence of cross-linking heterogeneities in the material, which are associated with a sticky behavior.

size resolution and then to export planar design geometries in a specific file format for the mask manufacturer, such as the Graphic Database System format (common acronym, GDS II).

Based on this design, a chrome-coated photomask in transparent fused silica or synthetic quartz is fabricated in a clean room. This photomask will permit to expose to ultraviolet (UV) light-specific regions of a thin layer of photoresist, beforehand spin coated onto a flat silicon substrate. The surface of the silicon substrate must be cleaned carefully to avoid the presence of defects that may induce the dewetting of the photoresist layer (Hamieh et al., 2007; Reiter et al., 2009). After UV photoillumination, the soluble photoresist is washed off using a liquid developer in order to obtain the photomask pattern made of cross-linked photoresist. At this stage, the silicon wafer coated with a thin layer of photoresist can be used as a topographic template for molding polydimethylsiloxane (PDMS) stamps (Fig. 3.2A). Alternatively, unprotected regions of the silicon master can be anisotropically etched, for instance by deep reactive-ion etching and then the photoresist stripped in order to obtain a more stable silicon template. The silicon master must be finally treated with the vapor of octadecyltrichlorosilane (or a perfluorosilane such as $C_6FI_3C_2H_5SiCl_3$) to cap

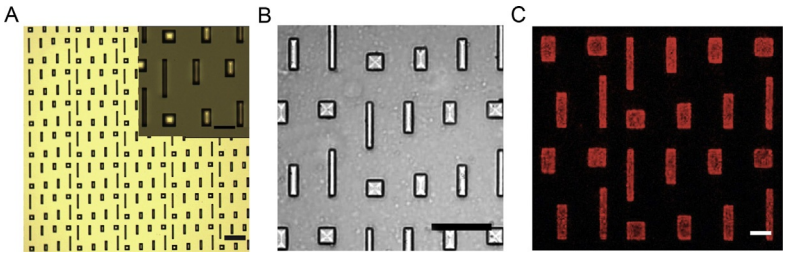

FIGURE 3.2

From the silicon master to protein micropatterns. (A) Optical micrograph of the surface of a silicon master structured with square-shaped and rectangular microscopic features. The inset shows a small zone of the silicon master. Scale bars are 200 μm for the master and 100 μm for the inset. (B) Optical micrograph of the surface of a silicone stamp obtained from the molding of the silicon master presented in (A). The scale bar is 100 μm. (C) Optical fluorescence image of different geometries of fibronectin micropatterns deposited by microcontact printing on a PDMS-coated coverslip ($E = 1$ MPa). The scale bar is 50 μm.

any polar reactive groups (e.g., –OH) present at the surface of the master with a chemically inert group such as $-CH_3$ or $-CF_3$.

A sylgard 184 prepolymer, which is a commercial silicon elastomer, with a 1:10 ratio of curing agent to base, is poured onto the silanized silicon master and then cured at 60 °C during 3 h to cross-link the polymer. Finally, the PDMS layer is peeled off from the template and stamps with a dimension of 10×10 mm^2 are cut with a scalpel. The stamps used for μCP are made of PDMS to mold with very high fidelity the microfeatures of the silicon master (Fig. 3.2B). Due to its elastomeric behavior, a PDMS stamp will deform enough to conform to the surface (Fig. 3.2C). In addition, the low surface energy of PDMS (~23 mJ/m^2) facilitates its separation from the silicon master and also to peel it easily from the printed surface.

3.2 MICROSTAMP FEATURES

Micropatterns were designed for studying at the single-cell level the effect of cell shape changes on the behavior of the nucleus. *In vivo*, endothelial cells reorientate and elongate in the direction of the blood shear stress. Low and oscillatory shear stress, that can be found in bifurcated and curved vessels, have been shown to be associated with a cobblestone-like shape of endothelial cells, whereas high and unidirectional shear stress were observed to induce elongated endothelial morphologies, up to an aspect ratio of 1:10. Consistent with these observations, we designed square (aspect ratio 1:1) and rectangular micropatterns with a wide range of aspect ratios (from 1:2 to 1:10) in order to reproduce *in vitro*, at the single-cell level, the different morphologies adopted *in vivo* by endothelial cells (Figs. 3.2C).

Interestingly, previous reports have demonstrated that the spreading area of adherent cells is a key parameter of the cell–substrate interactions (Yeung et al., 2005), suggesting that the spreading area is a parameter involved in the generation of intracellular forces that control the nuclear shape. Consistent with this observation, it can be therefore useful to investigate the role of the cellular morphology on the nuclear shape remodeling process by controlling the cell surface area. Previous reports have shown that mammalian cells need enough space to spread, whereas low spreading areas lead to apoptosis (Chen, Mrksich, Huang, Whitesides, & Ingber, 1997). In this work, each micropattern geometry was designed to adopt five values of areas: 600, 800, 1200, 1600, and 2000 μm^2 in order to decipher the role of the cell spreading area in the nuclear remodeling process. It is interesting to note that a gap of 50 μm was placed between micropatterns to prevent cell spreading on neighboring patterns.

3.3 SOFT MATRICES: HYDROXY-PAAm HYDROGELS

3.3.1 Materials

3.3.1.1 Reagents

Acrylamide in powder (Sigma-Aldrich, A3553)
N,*N*′-methylenebis(acrylamide) (Sigma-Aldrich, 146072)
N-hydroxyethylacrylamide (Sigma-Aldrich, 697931)
N,*N*,*N*′,*N*′-tetramethylenediamine (Sigma-Aldrich, T9281)
Sodium hydroxide (Sigma-Aldrich, 221465-25G)
Ammonium persulfate (APS) (Sigma-Aldrich, A3678)
Double-distillated water, ddH20
3-(trimethoxysilyl)propyl acrylate (Sigma-Aldrich, 1805)
Human plasma fibronectin (Millipore, FC010)
Laminin (Sigma-Aldrich, L2020)
Sterile phosphate buffered saline (PBS) (PAA Laboratories, H15-002).

3.3.1.2 Equipments

Laminar flow hood (Filtest Clean Air Technology)
Ultrasonic bath tray (Sigma-Aldrich, Z613983-1EA)
Vortexer (Scientific Industries, Vortex Genie 2)
Rocking plate (IKAcWerke, KS 130 Basic)
UV/Ozone Photoreactor (Ultraviolet Company, Model PR-100)
Vacuum degassing chamber (Applied Vacuum Engineering, DP-8-Kit)
Parafilm (Sigma-Aldrich, P7793-1EA)
Dressing tissue forceps (Sigma-Aldrich, F4391-1EA)
Polystyrene petri dishes (Sigma-Aldrich, P5731-500EA)
0.2 μm Isopore membrane filter (Millipore, GTTP Filter code)
22 mm round glass coverslip (Neuvitro, GG-22)
25 mm round glass coverslip (Neuvitro, GG-25)
Variable volume micropipette (Sigma-Aldrich, Z114820)

Microcentrifuge tubes (Sigma-Aldrich, Z666505-100EA)
75 cm^2 cell culture flask (Sigma-Aldrich, CLS430641)
Aluminum foil (Sigma-Aldrich, 266574-3.4G).

3.3.2 Method

3.3.2.1 Step #1: hydroxy-PAAm hydrogel fabrication

1. Place 25-mm-diameter glass circular coverslips in a petri dish and under a chemical fume hood smear 0.1 M NaOH solution on it for 5 min.
2. Drain the NaOH solution and fully immerse coverslips in sterile ddH_2O for 20 min under a gentle rocking.
3. Drain sterile ddH_2O and repeat step 2.
4. Remove coverslips with fine tweezers and place them in a new petri dish with the activated face up by squeezing a drop of sterile ddH_2O between the glass coverslip and the plastic petri dish.
5. Dry coverlips under a steady flow of high-purity nitrogen gas. The drop of sterile ddH_2O squeezed between the petri dish and the coverslip will avoid the coverslip to move.
6. In a culture hood, smear a thin layer of 3-(trimethoxysilyl)propyl acrylate (92%) on the activated side of the dried coverslips for 1 h.
7. Wash glass coverslips with three washes of sterile ddH_2O and then immerse them with sterile ddH_2O in a new petri dish.
8. Tap the petri dish with parafilm and place it on a rocker plate under gentle agitation for 10 min.
9. Remove the coverslips from ddH_2O with sterile tweezers and place them in a new petri dish with the activated face up.
10. Prepare 65 mg of *N*-hydroxyethyl acrylamide (HEA) in a 1.5 mL Eppendorf tube.
11. Add 1 mL of 50 mM sterile HEPES buffer to HEA and mix using a vortexer until the complete HEA dissolution.
12. Add 400 μL of 40% w/w in HEPES acrylamide solution and the required volume of 2% w/w in HEPES bis-acrylamide solution to reach the desired hydrogel stiffness (see Fig. 3.1A). Adjust with 50 mM HEPES to reach a final volume of 5 mL.
13. Mix the solution using a vortexer during 2 min and degas it in a vacuum chamber for 20 min. This step will permit to reduce the oxygen concentration within the solution that would prevent the polymerization of the hydroxy-PAAm solution.
14. Under a sterile hood, sterilize the degassed solution with a 0.2 μm pore size filter.
15. Activate 22-mm-diameter circular glass coverslips in a UV/Ozone cleaner during 7 min.
16. Prepare 100 μL of 10% APS solution, that is, 10 mg APS in 100 μL ddH_2O.

17. Add 2.5 μL of tetramethylenediamine (TEMED) and 25 μL of APS solution to the sterilized hydroxy-PAAm solution to initiate the polymerization. Under sterile conditions, mix the solution by three successive pipettings without introduction of bubbles.
18. Under a sterile hood, place a 25 μL drop of the hydroxy-PAAm solution on a 25-mm coverslip (from step 9) and immediately place a 22-mm glass coverslip (from step 15) on top of the droplet to squeeze the hydroxy-PAAm solution. Center the 22-mm glass coverslip with sterile tweezers and smooth out any bubbles.
19. Let hydroxy-PAAm hydrogels polymerize at room temperature for 15–30 min. Invert manually the remaining hydroxy-PAAm solution in the Eppendorf tube to follow the completion of the polymerization process.
20. Immerse coverslips in sterile ddH_2O and carefully separate the 22-mm glass coverslips by introducing the edge of a razor blade between the 22-mm glass coverslips and the hydroxy-PAAm hydrogel layer.
21. Wash with hydroxy-PAAm coated coverslips with three washes of sterile PBS.
22. Store hydroxy-PAAm hydrogels in sterile PBS at 4 °C for up to 3 days.

3.3.2.2 Step #2: Microcontact printing on hydroxy-PAAm hydrogels

1. Wash the PDMS microstamps by sonicating them for 15 min in a 70% solution of ethanol in water.
2. Dry the stamps with filtered nitrogen and place them in a petri dish with their microfeatures head-up.
3. Place the opened petri dish in a UV/ozone cleaner ($\lambda < 200$ nm) for 7 min.
4. Close the petri dish and bring it into the laminar flow hood.
5. Under sterile conditions, prepare a 25 μg/mL solution of fibronectin (or for instance a 100 μg/mL of laminin in PBS) in sterile water and spread 200 μL of this solution on the top of each stamp by moving it with a sterile tip of a pipette toward each corner of the stamp. Do not mix the fibronectin solution thoroughly.
6. Let the protein solution incubate on the stamps for 1 h at room temperature under the sterile hood. Turn off lamps to avoid protein damage.
7. Under a sterile hood, transfer hydroxy-PAAm coated coverslips into a new petri dish and remove excess PBS from the surface with a low nitrogen stream. Stop the procedure as soon as no evidence of standing water on the gel surface is observed. The gel should not be dried thoroughly at this stage.
8. Place the structured surface of the stamp in contact with the dried hydrogel surface. Ensure a good contact between the stamp and the hydrogel surface.
9. Leave the PDMS stamp on the hydrogel surface for 1 h at room temperature.
10. Gently remove PDMS stamps from hydroxy-PAAm hydrogels with forceps.
11. Under sterile conditions, wash extensively stamped hydroxy-PAAm hydrogels by three exchanges of PBS (pH 7.4) for 10 min per exchange and place them in a 6-well petri dish.

12. Passivate nonprinted zones by adding 3 mL/well of a sterile solution of Bovine Serum Albumin (BSA) at 5 mg/mL in PBS during one night at 4 °C under a gentle agitation on a rocking plate.
13. Wash extensively by three exchanges of PBS (pH 7.4) in sterile conditions for 10 min per exchange. At this stage, stamped hydroxy-PAAm hydrogels can be stored at 4 °C up to 1 week.

3.4 STIFF MATRICES: SILICONE ELASTOMERS

In this section, we describe the preparation of silicone elastomers with tunable rigidity and the procedure for micropatterning PDMS-coated coverslip with proteins from the ECM.

3.4.1 Materials

3.4.1.1 Reagents

Sylgard 184 silicone elastomer kit (Dow Corning)
Pluronic F127 Micropastille (BASF)
Petri dishes (Greiner bio one, 633102)
6-well culture plates (Greinerbio one, 657160)
25-mm-diameter glass coverslips (VWR, 631-1584)
Ethanol 99.8% (Sigma Aldrich, 02860)
Fibronectin from human plasma (Millipore, FC010)
Sterile PBS (PAA Laboratories, H15-002).

3.4.1.2 Equipments

UV/Ozone Photoreactor (Ultraviolet Products, model PR-100)
Rocking plate (IKAcWerke, Model KS 130 Basic)
Conditioning mixer (Thinky, ARE-250, USA)
Wafer spinner (Polos, MDC 300, The Netherlands)
Laminar flow hood (Filtest Clean Air Technology)
Ultrasonic bath (Sonoclean).

3.4.2 Method

3.4.2.1 Step #1: Fabrication of PDMS-coated coverslips

1. Round glass coverslips are cleaned by a 15-min sonication in a 70% solution of ethanol in water and dried with filtered nitrogen.
2. Prepare Sylgard 184 elastomer by mixing the PDMS monomer and its curing agent. A final elastic modulus ranging from 5×10^4 and 3×10^6 Pa can be obtained by adjusting the ratio (monomer:curing agent) between 40:1 and 10:1 (see Fig. 3.1B). In order to ensure a good mixing and degassing, the uncured

solution is placed in a conditioning mixer for 10 min. Alternatively, the mixture can be mixed manually during 10 min and then degassed under vacuum for 2 h.

3. Place a glass coverslip on a spin coater, then cover it with a drop of uncured PDMS elastomer and start the spin-coating program. In order to optimize the quality of the PDMS layer deposited, spin-coat with a speed gradually increasing from 500 to 5000 rpm, for a total duration of 2 min. Deposit the spin-coated coverslips in a petri dish.
4. Cure the PDMS layer by placing the petri dish containing the coated coverslips 3 h at 60 °C in an oven, regardless the value of the elastic modulus. Alternatively, let the coverslips cure for 24 h at room temperature.

3.4.2.2 Step #2: Microcontact printing on PDMS-coated coverslips

1. Wash the PDMS microstamps by sonicating them for 15 min in a 70% solution of ethanol in water.
2. Dry the stamps with filtered nitrogen and place them in a petri dish with their microfeatures head-up.
3. Place the opened petri dish in a UV/ozone cleaner ($\lambda < 200$ nm) oven for 7 min.
4. Close the petri dish and bring it into the laminar flow hood.
5. Under sterile conditions, prepare a 25 μg/mL solution of fibronectin (or any other ECM proteins such as laminin or collagen) in sterile water and spread 400 μL of this solution on the top of each stamp. Do not mix the fibronectin solution thoroughly.
6. Let the fibronectin solution incubate on the stamps for 1 h at room temperature under the sterile hood.
7. Prepare a 1% w/w solution of Pluronic F 127 in water. Filter this solution with a 0.20-μm pore size filter in order to sterilize it.
8. About 10 min before the end of the incubation time, place the PDMS-coated coverslips in the UV/ozone and treat them for 7 min. Close the petri dish and bring it into the laminar flow hood.
9. Dry the stamps with filtered nitrogen under the laminar flow hood.
10. Place a stamp head-down on an activated PDMS-coated coverslip for 30 s.
11. With sterile forceps, remove the stamp from the coverslip and place the stamped coverslips in a 6-well culture plate.
12. Add 4 mL of the Pluronic solution on the wells during 5 min in order to passivate the unfunctionalized regions of the coverslip.
13. Rinse three times with 4 mL of sterile PBS. The microcontact printed coverslips can be used immediately or stored in sterile PBS at 4 °C for up to 1 week.

3.5 CELL DEPOSITION

This part describes the method used to control the shape of single Human Umbilical Vein Endothelial Cells (HUVECs) by deposing protein micropatterns on PDMS surfaces, as shown in Versaevel et al. (2012), and hydroxy-PAAm surface, as shown in

Grevesse et al. (2013). These methods have been used successfully in our laboratory with the following cell types: primary cortical neurons, normal human dermal fibroblasts, ECV 304, bone osteosarcoma cells (MG-63 cell line), human osteosarcoma-derived cells (SaOs-2), human osteoprogenitor (HOP), and human skeletal myoblasts (LHCN M2).

3.5.1 Materials

3.5.1.1 Reagents

PBS (PAA Laboratories, HIS-002)
Trypsin (0.5 g/L)–ethylenediaminetetraacetic acid (EDTA) (0.2 g/L) (Invitrogen/Gibco, 25300-054)
Endothelial cell growth medium (Cell Applications, 211 K-500)
Fetal bovine serum (PAA Laboratories, AIS_ISI)
Penicillin–streptomycin (Invitrogen/Gibco, 15140-122)
HUVECs (Invitrogen, C-003-5C)
Absolute ethanol (Sigma-Aldrich, 459844-2.5 L).

3.5.1.2 Equipments

Laminar Flow hood (Filtest Clean Air Technology)
75-cm^2 cell culture flask (Sigma-Aldrich, CLS430641)
Protein microcentrifuge tubes (Sigma-Aldrich, Z666505-100EA)
Cell incubator (Binder, APT line C150)
Centrifuge (Hermle, Z 252 MK)
Stainless steel forceps with fine tips (Sigma Aldrich, Z225304-1EA)
Cell culture multidish six wells (Sigma Aldrich, Z688649-4CS)
Variable volume micropipette (Sigma-Aldrich Z114820)
Sterile pipettes (Sigma-Aldrich, CLS70785N).

3.5.2 Method

1. Incubate PDMS or hydroxy-PAAm-coated coverslips in sterile culture medium at 37 °C for 30–45 min prior to plating cells.
2. Wash adherent cells cultured in a 75-cm^2 culture flask with sterile PBS at 37 °C and then detach cells with 3 mL of trypsin–EDTA or accutase for 10 min.
3. Transfer the desired amount of prewarmed complete growth medium appropriate for your cell line into the flask containing the detached cells and transfer the cell suspension into a tube for centrifugation.
4. Centrifuge the cell suspension for 3 min at 2000 rpm.
5. Under a sterile hood, remove the supernatant with a micropipette and resuspend the cells in complete culture medium (37 °C) at 15–20,000 cells/mL.
6. Place coverslips obtained from Step #1 in a cell culture multidish.
7. Add 4 mL of the cell solution in a well and place the multidish plate in a culture incubator at 37 °C and 5% humidity for 1–2 h.

8. Under a sterile hood, gently aspirate unattached cells and replace the culture medium with a fresh warmed one.
9. Return the attached cells to the incubator and let them spread onto the micropatterned surface (3–6 h, depending on the cell type).

3.6 DISCUSSION

Several types of polymer can be used to fabricate matrix substrates of varying stiffness. Here, we introduce two simple methods to create matrices of tunable elasticity by using hydroxy-PAAm hydrogels and Sylgard 184 silicone elastomers. Both polymers offer several important advantages for cell culture, such as constant surface chemistry in their working range of mechanical properties, translucent quality for optical and fluorescence microscopy, and compatibility with the micropatterning technique. As shown in Fig. 3.3, the complementarity of "soft" hydroxy-PAAm hydrogels and "stiff" Sylgard 184 silicone elastomers allows to obtain a three order-of-magnitude range of tunability that permits to recapitulate the whole range of stiffnesses (from ~1 kPa to ~1 MPa) observed for cells and tissues.

By combining the microcontact printing technique with both materials, we have investigated the role of the matrix stiffness on the regulation of the nucleus. Indeed, orientation and deformation of the nucleus are regulated by lateral compressive forces, which are driven by accumulated tension in central actin fibers (Versaevel et al., 2012). By changing the substrate stiffness over three orders of magnitude,

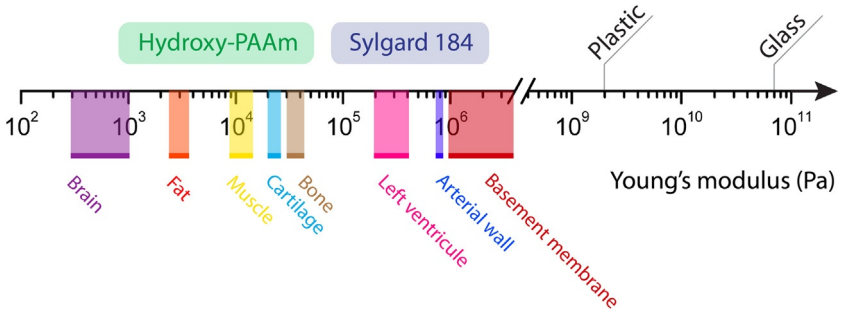

FIGURE 3.3

Soft tissue elasticity scale ranging from soft brain, fat, striated muscle, cartilage, and precalcified bone to left ventricule at peak systole and arterial walls. In contrast, conventional culture surfaces, such as plastic dishes and glass coverslips, exhibit much stiffer elastic moduli (~2×10^9 and ~7×10^{10} Pa, respectively). The top part of the panel shows the range of elastic moduli available with hydroxy-PAAm hydrogels (in green) and the sylgard 184 silicone elastomer (in blue).

we have studied whether significant modifications of the matrix stiffness can impact the nuclear shape by changing the level of tension in actin stress fibers. Considering that large variations of the spreading area have been observed previously in response to matrix stiffness modifications, we plated single HUVECs on rectangular fibronectin (FN)-coated micropatterns with a constant area of 1200 μm^2. This procedure permits to control in the same assay spreading and morphology of single HUVECs. These FN micropatterns were deposited on hydroxy-PAAm hydrogels of 2.5, 8.5, and 25 kPa and silicone elastomers of 1 MPa. It is important to note that fluorescent assays performed on these four substrates have shown a similar surface chemistry, regardless of the polymer nature and the rigidity value. Therefore, by controlling (i) the cellular shape, (ii) the spreading area, and (iii) the protein coating, we ensure that any eventual modifications of the nuclear shape will be directly related to changes in the matrix stiffness. After 24 h in culture, HUVECs were fixed and immunostained to observe the spatial distribution of actin filaments, focal adhesions, and the shape of the nucleus (Fig. 3.4).

We observed that cells plated on stiffer substrates had thicker and straighter actin fibers, a more deformed nucleus, and well-defined focal adhesion areas. These observations indicate that modifications of the cell matrix stiffness can impact the nucleus without changing the cellular shape, the cell–substrate adhesion, or the spreading area.

This suggests that changes of matrix rigidity modulate the production of internal tension in actin fibers, which result in a remodeling of the nucleus. By using morphometric analysis of the nucleus, we demonstrated that the projected nuclear area decreased significantly with the substrate stiffening. As shown in Fig. 3.5A, we observed a decrease of ~52% from 2.5 kPa to 1 MPa. Then, we quantified the nuclear

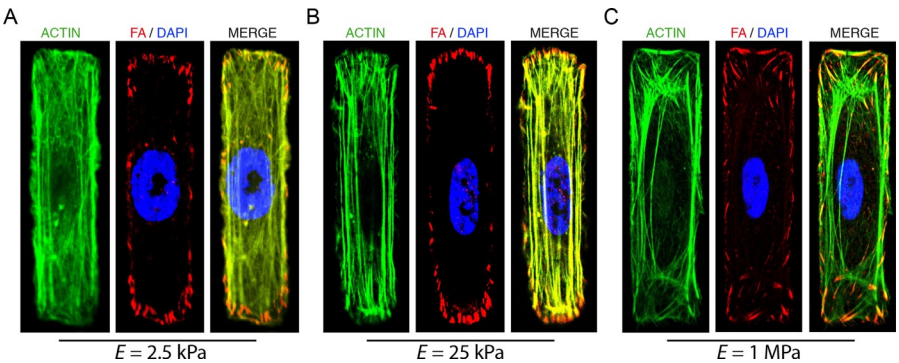

FIGURE 3.4

Immunostained HUVECs cultured on rectangular FN-coated micropatterns (aspect ratio 1:4) deposited on (A) $E = 2.5$ kPa, (B) $E = 25$ kPa hydroxy-PAAm hydrogels, and (C) 1 MPa silicone elastomers.

Reproduced from Grevesse et al. (2013) by permission of The Royal Society of Chemistry.

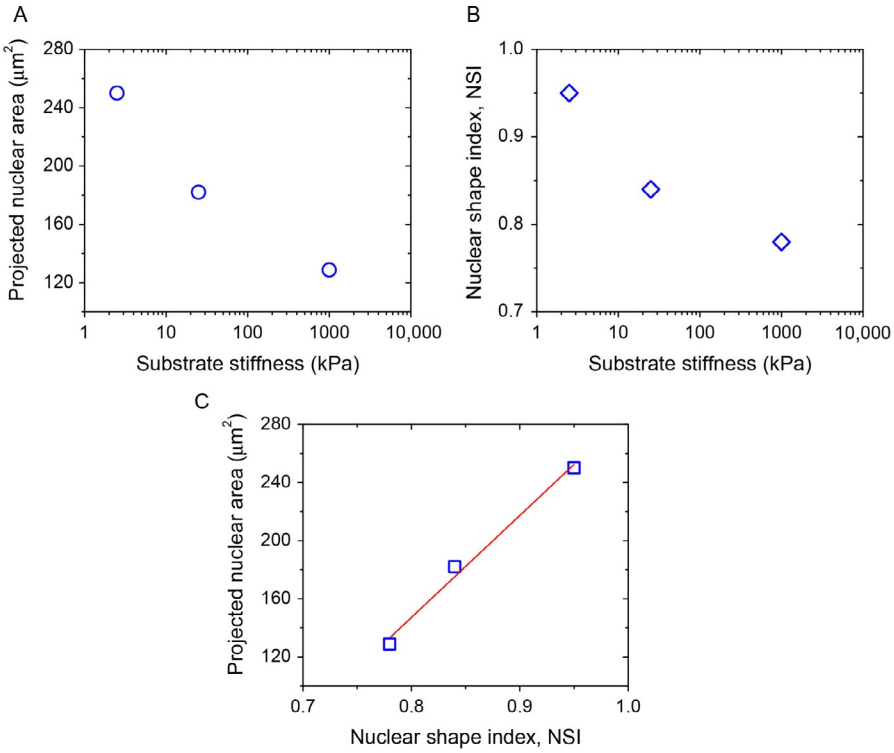

FIGURE 3.5

Morphometric evolution of the nucleus of single HUVECs cultured on rectangular-FN micropatterns (aspect ratio 1:4) that were deposited on 2.5 and 25 kPa hydroxy-PAAm hydrogels and 1 MPa silicone elastomers. Evolution of (A) the projected nuclear area versus the substrate stiffness in semilogarithmic scale, (B) the nuclear shape index versus the substrate stiffness in a semilogarithmic scale, and (C) the projected nuclear area as a function of the nuclear shape index. The red line corresponds to a linear fit ($R^2 = 0.997$).

shape by introducing a nuclear shape index, such as: $\text{NSI} = (4 \times \pi \times \text{area})/\text{perimeter}^2$. We show that NSI decreased from ~0.95 to ~0.78 when HUVECs were plated on substrate of 2.5 kPa and 1 MPa, respectively, suggesting a large deformation of the nucleus on stiffer culture substrates (Fig. 3.5B). Interestingly, we demonstrated that the dependences of the nuclear area and NSI on the matrix stiffness are intimately linked, as observed by the linear relation in Fig. 3.5C. These results show that modifications of the cell matrix rigidity can significantly impact the nucleus without affecting other cellular parameters, such as shape, substrate adhesion, or spreading area.

GENERAL CONCLUSIONS

We have reported two microcontact printing methods on hydroxy-PAAm hydrogels and Sylgard 184 silicone elastomers for creating "soft" and "stiff" functionalized biomaterials, over three orders of magnitude. These methods, which are based on commercially available and low-cost polymers, do not require special equipment or specific expertize. We hope that these methods will permit biologists and biophysicists to tune easily the elastic moduli of biomaterials in order to decouple the effect of mechanotransduction cues such as matrix stiffness, cell shape, or spreading area on cell fate.

Acknowledgments

This work was supported by the Belgian National Foundation for Scientific Research (F.R.S.-FNRS) through "MIS Confocal Microscopy," "Crédit aux Chercheurs" grants, and the "Nanomotility FRFC project" (no. 2.4622.11). T.G. doctoral fellowship is supported by the Foundation for Training in Industrial and Agricultural Research (FRIA). M.R. is Research Fellow of the F.R.S.-FNRS.

References

Brock, A., Chang, E., Ho, C. C., LeDuc, P., Jiang, X., Whitesides, G. M., et al. (2003). Geometric determinants of directional cell motility revealed using microcontact printing. *Langmuir*, *19*, 1611–1617.

Chen, C. S., Mrksich, M., Huang, S., Whitesides, G. M., & Ingber, D. E. (1997). Geometric control of cell life and death. *Science*, *276*, 1425–1428.

Engler, A. J., Sen, S., Sweeney, H. L., & Discher, D. E. (2006). Matrix elasticity directs stem cell lineage specification. *Cell*, *126*, 677–689.

Gabriele, S., Benoliel, A.-M., Bongrand, P., & Théodoly, O. (2009). Microfluidic investigation reveals distinct roles for actin cytoskeleton and myosin II activity in capillary leukocyte trafficking. *Biophysical Journal*, *96*, 4308–4318.

Gabriele, S., Versaevel, M., Preira, P., & Théodoly, O. (2010). A simple microfluidic method to select, isolate, and manipulate single-cells in mechanical and biochemical assays. *Lab on a Chip*, *10*, 1459–1467.

Gao, L., McBeath, R., & Chen, C. S. (2010). Stem cell shape regulates a chondrogenic versus myogenic fate through Rac1 and N-cadherin. *Stem Cells*, *28*, 564–572.

Guilak, F., Cohen, D. M., Estes, B. T., Gimble, J. M., Liedtke, W., & Chen, C. S. (2009). Control of stem cell fate by physical interactions with the extracellular matrix. *Cell Stem Cell*, *5*, 17–26.

Grevesse, T., Versaevel, M., Circelli, G., Desprez, S., & Gabriele, S. (2013). A simple route to functionalize polyacrylamide hydrogels for the independent tuning of mechanotransduction Cues. *Lab on a Chip*, *13*, 777–780.

Hamieh, M., Al Akhrass, S., Hamieh, T., Damman, P., Gabriele, S., Vilmin, T., et al. (2007). Influence of substrate properties on the dewetting dynamics of viscoelastic polymer films. *Journal of Adhesion*, *83*, 367–381.

Jaalouk, D. E., & Lammerding, J. (2009). Mechanostransduction gone awry. *Nature Review Molecular Cell Biology*, *10*, 63–73.

Kwon, M., Godinho, S. A., Chandhok, N. S., Ganem, N. J., Azioune, A., Théry, M., et al. (2008). Mechanisms to suppress multipolar divisions in cancer cells with extra centrosomes. *Genes Development*, *22*, 2189–2203.

Lecuit, T., & Lenne, P. F. (2007). Cell surface mechanics and the control of cell shape, tissue patterns and morphogenesis. *Nature Review Molecular Cell Biology*, *8*, 633–644.

Palchesko, N. P., Zhang, L., Sun, Y., & Feinberg, A. W. (2012). Development of polydimethylsiloxane substrates with tunable elastic modulus to study cell mechanobiology in muscle and nerve. *PLoS One*, *7*, e51499.

Pathak, A., & Kumar, S. (2012). Independent regulation of tumor cell migration by matrix stiffness and confinement. *Proceedings of the National Academy of Sciences of the United States of America*, *109*, 10334–10339.

Pelham, R. J., Jr., & Wang, Y. (1997). Cell locomotion and focal adhesions are regulated by substrate flexibility. *Proceedings of the National Academy of Sciences of the United States of America*, *94*, 13661–13665.

Reiter, G., Al Akhrass, S., Hamieh, M., Damman, P., Gabriele, S., Vilmin, T., et al. (2009). Dewetting as an investigative tool for studying properties of thin polymer films. *European Physical Journal: Special Topics*, *166*, 165–172.

Solon, J., Levental, I., Sengupta, K., Goerges, P. C., & Janmey, P. A. (2007). Fibroblast adaptation and stiffness matching to soft elastic substrates. *Biophysical Journal*, *93*, 4453–4461.

Théry, M. (2010). Micropatterning as a tool to decipher cell morphogenesis and functions. *Journal of Cell Science*, *123*, 4201–4213.

Théry, M., Racine, V., Pépin, A., Piel, M., Chen, Y., Sibarita, J. B., et al. (2005). The extracellular matrix guides the orientation of the cell division axis. *Nature Cell Biology*, *7*, 947–953.

Thomas, C. H., Collier, J. H., Sfeir, C. S., & Healy, K. E. (2002). Engineering gene expression and protein synthesis by modulation of nuclear shape. *Proceedings of the National Academy of Sciences of the United States of America*, *99*, 1972–1977.

Versaevel, M., Grevesse, T., & Gabriele, S. (2012). Spatial coordination between cell and nuclear shape within micropatterned endothelial cells. *Nature Commununications*, *3*, 671.

Versaevel, M., Grevesse, T., Riaz, M., & Gabriele, S. (2013). Nuclear confinement: Putting the squeeze on the nucleus. *Soft Matter*, *9*, 6665–6676.

Wang, N., Tytell, J. D., & Ingber, D. E. (2009). Mechanotransduction at a distance: Mechanically coupling the extracellular matrix with the nucleus. *Nature Review Molecular Cell Biology*, *10*, 75–82.

Yeung, T., Georges, P. C., Flanagan, L. A., Marg, B., Ortiz, M., Funaki, M., et al. (2005). Effects of substrate stiffness on cell morphology, cytoskeletal structure, and adhesion. *Cell Motility and the Cytoskeleton*, *60*, 24–34.